usenix THE ADVANCED COMPUTING SYSTEMS ASSOCIATION

Increasing Adversarial Uncertainty to Scale Private Similarity Testing

Yiqing Hua and Armin Namavari, *Cornell Tech and Cornell University;*
Kaishuo Cheng, *Cornell University;* Mor Naaman and Thomas Ristenpart,
Cornell Tech and Cornell University

https://www.usenix.org/conference/usenixsecurity22/presentation/hua

This paper is included in the Proceedings of the
31st USENIX Security Symposium.

August 10–12, 2022 • Boston, MA, USA

978-1-939133-31-1

Open access to the Proceedings of the
31st USENIX Security Symposium is
sponsored by USENIX.

Increasing Adversarial Uncertainty to Scale Private Similarity Testing

Yiqing Hua[1,2], Armin Namavari[1,2], Kaishuo Cheng[2], Mor Naaman[1,2], Thomas Ristenpart[1,2]
[1] *Cornell Tech* [2] *Cornell University*

Abstract

Social media and other platforms rely on automated detection of abusive content to help combat disinformation, harassment, and abuse. One common approach is to check user content for similarity against a server-side database of problematic items. However, this method fundamentally endangers user privacy. Instead, we target client-side detection, notifying only the users when such matches occur to warn them against abusive content.

Our solution is based on privacy-preserving similarity testing. Existing approaches rely on expensive cryptographic protocols that do not scale well to large databases and may sacrifice the correctness of the matching. To contend with this challenge, we propose and formalize the concept of similarity-based bucketization (SBB). With SBB, a client reveals a small amount of information to a database-holding server so that it can generate a bucket of potentially similar items. The bucket is small enough for efficient application of privacy-preserving protocols for similarity. To analyze the privacy risk of the revealed information, we introduce a framework for measuring an adversary's confidence in inferring a predicate about the client input correctly. We develop a practical SBB protocol for image content, and evaluate its client privacy guarantee with real-world social media data. We then combine SBB with various similarity protocols, showing that the combination with SBB provides a speedup of at least 29× on large-scale databases compared to that without, while retaining correctness of over 95%.

1 Introduction

Faced with various policy-violating activities ranging from disinformation [59] to harassment [21, 34, 48] and abuse [10, 73], social media companies increasingly rely on automated algorithms to detect deleterious content. One widely used approach is to check that user content is not too similar to known-bad content. For example, to detect child sexual abuse imagery [10], some platforms utilize similarity hashing approaches like PhotoDNA [51] or PDQHash [1]. These approaches map user-shared images into unique representations that encode perceptual structure, enabling quick comparisons against a database of hash values. Such approaches could be helpful for combating other forms of bad content, such as the viral spread of visual misinformation on end-to-end encrypted messaging services [59]. For example, they could augment other efforts to provide users with important context about shared content [5, 16].

Currently deployed approaches rely on sending user content or a similarity hash of the content to a moderation service. This risks user privacy. As we detail in the body, the service can easily match a submitted similarity hash against known images to learn the content of a user's image with overwhelming confidence. Privacy can be improved utilizing cryptographic two-party computation (2PC) [42, 77] techniques to only reveal matching content to the moderation service and nothing more. The recent CSAM image detection system proposed by Apple [3] goes one step further and notifies the platform only when the number of matching images surpasses a certain threshold. Automated notification of platforms necessarily raises concerns about privacy and accountability (e.g., how to ensure the system is not used for privacy-invasive search for benign images).

An alternative approach is to have only the client learn the output of similarity checks, to enable client-side notifications, warning or otherwise informing users. This may not be suitable for all classes of abusive content, such as CSAM, where the recipient may be adversarial, but could be useful for other abuse categories (misinformation, harassment, etc.). However, the scale of databases makes it prohibitive both to send the known-bad hashes to the client or, should hashes be sensitive, apply 2PC techniques to ensure as little as possible about the database leaks to clients. For an example of the latter, Kulshrestha and Mayer's [42] private approximate membership computation (PAMC) protocol achieves state-of-the-art performance, but nevertheless requires about 27 seconds to perform a similarity check against a database with one million images. The protocol also has an average false negative rate of almost 17% for slightly transformed images, meaning many similar images may be erroneously marked as dissimilar.

In this work, we target client-side detection, in order to warn users against abusive content. To this end, we explore the question of how to scale privacy-preserving image similarity protocols, while preserving correctness of the similarity testing. We introduce and formalize the concept of similarity-based bucketization (SBB). The idea is to reveal a small amount of structured information in a message to a database-holding server, so that it can determine a bucket of possibly relevant database entries. Ideally the bucket consists of only a small fraction of the full database, enabling use of a subsequent similarity testing protocol on the bucket to perform the final similarity check. We explore instantiating the testing protocol in a variety of ways.

The key technical challenge facing SBB is balancing the competing goals of minimizing bucket size (efficiency) with leaking as little information as possible (privacy). For example, one could modify a standard similarity hash, say PDQHash, to provide only very coarse comparisons. But as we will show, this still leaks a lot of information to the server, allowing high-confidence attacks that can associate the coarse hash to the specific content of a client request. More broadly we need a framework for navigating this tension.

We propose such a framework. It formalizes information leakage using a game-based definition. To be specific, an adversarial server attempts to learn, from an SBB message generated for some image drawn from an adversary-known distribution, a predicate about the underlying image. As an important running example, we use a "matching predicate" that checks if the underlying image has the same perceptual hash value as that of a known target image. Unlike in more traditional cryptographic definitions (e.g., [30]), we do not require the adversarial server to have negligible success (which would preclude efficiency) and instead offer a range of measures including accuracy improvement over baseline guessing, adversarial precision, and adversarial area under the receiver operating characteristic curve (AUC). Indeed, there is no one-size-fits-all approach to measuring privacy damage, and our framework allows one to more broadly assess risks.

We offer a concrete SBB mechanism that increases adversarial uncertainty compared to naive approaches. It converts any similarity hash that uses Hamming distance to a privacy-preserving coarse embedding; we focus on PDQHash because it is widely supported. We combine techniques from locality-sensitive hashing [29] with lightweight noise mechanisms. The ultimate algorithm is conveniently simple: apply a standard PDQHash to an image, choose a designated number d of bit indices randomly, flip each selected bit with probability γ, and then send the resulting d bits and their indices to the server. An image in the server's database is included in a bucket should k or fewer of the relevant d bits of its PDQHash mismatch with those that are sent from the client.

Using real-world social media data, we empirically assess correctness, efficiency and privacy under various definitions. We explore various settings of d, γ, and k, and show that it is possible to ensure average bucket sizes of 9.3% of the database, while: (1) ensuring that the similar images are included in the bucket at least 95% of the time, and (2) an optimal adversary for the matching predicate achieves less than 50% precision, signifying low confidence in matching attacks. We caution that these empirical results are dataset-dependent, and may not generalize to every potential use case. Instead they can be interpreted as a proof-of-concept that SBB works in a realistic scenario.

We then combine our SBB mechanism with various similarity protocols, with different privacy guarantees for the server's content. For the expedient approach of downloading the bucket of server PDQHash values and performing comparisons on the client side, SBB provides a speedup of 29$\times$ or more. A full similarity check requires less than 0.5 seconds for a database of 2^{23} images. We also explore using SBB to speed up an ad hoc similarity protocol based on secure sketches [20], as well as 2PC protocols implemented in the EMP [72] and CrypTen [41] frameworks. Our experiments indicate that SBB can provide speed-ups of 601$\times$, 97$\times$, and 67$\times$, respectively, and often enables use of 2PC that would fail otherwise due to the size of the database.

We conclude by discussing various limitations of our results, and open questions that future work should answer before deployment in practice. Nevertheless, we expect that our SBB approach will be useful in a variety of contexts. Encrypted messaging apps could use it to help warn users about malicious content, with significantly better privacy than approaches that send plaintext data to third-party servers [5,16]. In another setting, social media platforms that currently query their users' plaintext data to third-party services to help identify abuse (e.g., [26,69]) could use our techniques to improve privacy for their users. To facilitate future research, our prototype implementation is publicly available.[1]

2 Background and Existing Approaches

In this section, we provide some background about a key motivating setting: providing client-side detection of bad content in end-to-end (E2E) encrypted messaging. That said, our approaches are more general and we discuss other deployment scenarios in the extended version [35].

Content detection and end-to-end encryption. Content moderation aims to mitigate abuse on social media platforms, and can include content removal, content warnings, blocking users, and more. Most moderation approaches rely on detecting objectionable content, particularly at scale where automated techniques seem to be requisite. Social media companies often maintain large databases of known adversarial content [10,51] and compare a client message with items in

[1] https://github.com/vegetable68/sbb

the databases to see if the message is sufficiently similar to some piece of adversarial content. However, this approach requires the client to reveal plaintext message content, which stands in tension with privacy-preserving technologies like E2E encryption. On the other hand, leaving contents unmoderated on the platform is unsatisfactory given the harms caused by abusive content such as misinformation, child sexual abuse material (CSAM), harassment, and more.

Governments[2] and non-governmental organizations[3] have for many years emphasized the need for technical innovations that could enable law enforcement access to encrypted data, while minimizing risks of privacy violation [2, 23, 63]. However, security experts have repeatedly expressed concern that such 'backdoor' access would fundamentally break the privacy of E2E encryption [18,40,52,57] or, if it provided content blocking functionality, enable problematic censorship [57].

In this work, we target mitigations that allow privacy-preserving client-side detection of content similar to known bad content. We focus on images, as discussed below. Our protocol is agnostic to how client software uses this detection capability, but we believe that client software should be designed to empower users with information and the ability to make their own decisions about content.

Our techniques may be useful, for example, to mitigate the increasing use of E2E encrypted messaging for harmful disinformation campaigns [32, 59]. A widely discussed approach is to warn users against known disinformation. Recent research [39] has shown that when carefully designed, such warnings are effective in guiding user behaviors to avoid disinformation. Our work provides a technical solution for the client-side warning mechanism. To be specific, the proposed system queries whether a client's received content is similar to known disinformation and returns the answer only to the client. Such a design avoids both outright censorship and notifying platform operators that a particular client received a particular piece of content. This solution would enable the kinds of user-initiated known content detection approaches that have been suggested recently [11, 49], and could help complement existing anti-abuse techniques that do not consider content, such as those used in WhatsApp [74].

But warning-style approaches that inform and empower users may not be suitable for threats like CSAM, where the recipients of messages can themselves be bad actors. Here client software would seemingly have to limit user choice, automatically blocking detected content and/or notifying some authority about it. Recent designs for CSAM mitigations include the Kulshrestha-Mayer protocol [42] (when used to notify the platform) and the CSAM detection proposal by Apple [3]. Cryptographers have, in turn, raised the alarm that, while efforts to combat CSAM are laudable, these platform-notifying systems represent a potential E2E encryption backdoor that is subject to misuse by platform operators or governments [31, 50] and that future work is needed to make such systems transparent and accountable. Our work is different, as we target client-side notification and not platform notification.

Another concern is that even client-side notification ends up a stepping stone towards riskier backdoor/censorship mechanisms, because once the former is deployed it will be easier to deploy, or justify deploying, the latter. Client-side functionality at least provides the opportunity for activists and others to detect changes to client-side software and understand their effects, adding some transparency and accountability. At the same time, arguments for, or against, various anti-abuse mechanisms would do well to delineate between approaches that empower users to understand and control their online experience (warnings, the ability to select users/content to block) and that disempower users (client-side or platform-side automatic censorship). We believe our techniques will be useful for the former, without intrinsically promoting the latter.

Client-side similarity testing and privacy. As mentioned above, we focus on private image similarity testing services. These allow a client, who receives some value w on an E2E encrypted platform, to submit a request to a service provider holding a database $\mathcal{B}$; the response indicates to the client whether w is similar to any item in $\mathcal{B}$. As the database $\mathcal{B}$ may be quite large, we need scalable solutions. The service provider could be the messaging platform, or a third party service. In the case when the provider is a third party service, the protocol runs between the client and the testing service, without involvement of platform servers.

A key concern will be the privacy risk imposed on clients by a testing service. Our threat model consists of an adversary in control of the service's servers, who wants to learn information about a client's image w by inspecting messages sent to the service in the course of similarity testing. This is often referred to as a semi-honest adversary, though our approaches will meaningfully resist some types of malicious adversaries that deviate from the prescribed protocol. In terms of privacy threat, we primarily focus on what we call a matching attack, in which the adversary wishes to accurately check whether w matches some adversarially chosen image (see Section 4 for a formalization). A matching attack enables, for example, adversarial service operators to monitor whether clients received any image on an adversarially chosen watchlist.

In this initial work we primarily focus on the risks against a single query from the client, and explicitly do not consider adversaries that just want to recover partial plaintext information, such as if the adversary wants to infer if an image contains a person or not. While we believe our results also improve privacy for such attacks, we do not offer evidence either way and future work will be needed to explore such threats. We also do not consider misbehaving servers that seek to undermine correctness, e.g., by modifying $\mathcal{B}$ to force clients to erroneously flag innocuous images. How to build accountability mechanisms for this setting is an interesting

[2] https://www.justice.gov/opa/press-release/file/1207081
[3] https://www.missingkids.org/e2ee

open question. We simulate the scenarios of adversaries that somehow can take advantage of known correlations between queried images in the extended version [35] and propose potential mitigation solutions in Section 7.

Nevertheless there are already several challenges facing developing a service that prevents accurate matching attacks in our setting. While prior work has established practical protocols for private set membership [43, 70], these only provide exact equality checks. Even small manipulations such as image re-sampling, minor cropping, or format conversion make exact matching schemes fail. Second, the database $\mathcal{B}$ can be arbitrarily large and may require frequent update. For instance, the published dataset from Twitter with activities of accounts associated to the Russian Internet Research Agency consist of 2 million images in total [28].

Existing approaches. We review deployed systems and suggested designs for image similarity testing.

Plaintext services. Most current deployments have the client upload their image to a third party service. A prominent example is the PhotoDNA service. After a client submits an image to the service, it immediately hashes the image using a proprietary algorithm [51]. Importantly, the hash can be compared to other hashes of images in a way that measures similarity of the original images. Such hashes are often called similarity hashes [15, 54] or perceptual hashes [78]. (We show examples later.) The original image that was sent to the service is deleted after hashing. This plaintext design has various benefits, including simplicity for clients and the ability to hide the details of the hashing used. The latter is important in contexts where malicious users attempt to modify an image $w \in \mathcal{B}$ in the service's bad list to create an image w' that will not be found as similar to any image in $\mathcal{B}$ (including w) [76].

Another example of a plaintext service is WhatsApp's in-app reverse search function to combat visual misinformation [5], rolled out in June 2020. This feature allows users to submit their images to Google reverse image search for the source or context of a specific image. In this case, the user needs to reveal their image to both Google and WhatsApp, sacrificing user privacy.

Hashing-based services. For privacy-aware clients, revealing plaintext images represents a significant privacy risk. An alternative approach is to use a public hashing algorithm, have the client first hash their image, and submit only the resulting representation to the similarity checking service. While this requires making the hashing algorithm available to clients (and, potentially, adversarial users), it improves privacy because the original images are not revealed to the service. It also improves performance: hashes can be compact (e.g., 256 bits) and compared against a large database $\mathcal{B}$ in sublinear time [53]. This approach is used by Facebook's ThreatExchange [26] service that allows organizations to share hashes of images across trust boundaries. They use a custom similarity hash called PDQHash [1].

Sharing hashes, however, still has privacy risk. For example, although the lossy process of PDQHash generation makes recovering the exact input impossible in general, revealing the hash allows inferring whether a queried value is similar to another image. An adversary at the service provider's side may brute-force search a database of images to find ones close to the queried value.

Cryptography-based services. An alternative approach that preserves privacy is to employ a secure 2PC protocol [77] between the client and service. Existing 2PC protocols for similarity matching (e.g., [7, 13, 37]) can, in the best case, ensure that no information about the client's image is leaked to the server and that nothing about $\mathcal{B}$ (beyond whether it contains a similar image) leaks to the client. However, existing 2PC protocols do not efficiently scale to large databases $\mathcal{B}$.

Recent work by Kulshrestha and Mayer [42] proposed private approximate membership computation (PAMC) to allow similarity testing of images encoded as PDQHashes. The protocol begins by splitting the database $\mathcal{B}$ into buckets. Using private information retrieval, a client retrieves a bucket from the server with the bucket identifier generated from the PDQHash of their image. The chosen bucket is not disclosed to the server. The two parties then perform a private similarity test to determine whether the client PDQHash has sufficiently small Hamming distance to any image in the bucket. The protocol is still rather expensive, with their initial experiments requiring 37.2 seconds for a one-time set up and 27.5 seconds for a query for a block list with the size of 2^{20}. These times exclude network delays (measurements were performed with client and server on the same workstation). While a step closer to practicality, this remains prohibitive particularly since we expect that performance in deployment would be worse for lightweight client hardware such as mobile phones.

Concurrent work by Apple [3] proposed a protocol that encodes images from a user's cloud storage into perceptual hashes. The perceptual hashing algorithm maps similar images into identical hashes with high probability. The protocol then performs private set intersection between the encoded hashes and a database of known CSAM images. The private contents are revealed to the platform only when the number of matches exceeds a certain threshold. Whether such a protocol, designed for CSAM detection, is fit for client-side detection remains a question for future work to explore.

In summary, all three existing design approaches for image similarity testing — revealing images as client requests, using similarity representations like PDQHash as client requests, and employing secure 2PC protocols — do not provide satisfying solutions. The first two designs do not provide sufficient privacy, while 2PC designs are currently not sufficiently efficient. Thus we need a new approach to similarity testing.

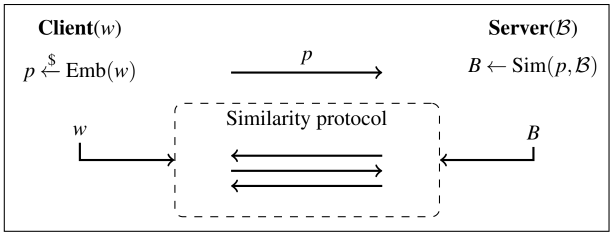

Figure 1: Two-stage framework for using similarity-based bucketization to determine if an image w is similar to one in an image dataset $\mathcal{B}$.

3 Similarity-Based Bucketization

To enable efficient, privacy-preserving client-side similarity testing, we take inspiration from previous work that used bucketization to support efficient private set membership testing [43, 70]. These will, however, not work for image similarity testing. We therefore introduce a new two-step framework, as shown in Figure 1. It first enables scaling by utilizing what we call similarity-based bucketization (SBB) to gather a subset $B \subseteq \mathcal{B}$, called a bucket, of possibly relevant images. The second step is to perform a similarity testing protocol over the bucket; we explore how SBB can provide scaling improvements for several different similarity testing protocols. In this section we introduce coarse embeddings, which allow crude similarity comparisons, rather than the granular ones that regular similarity hashes provide. A summary of the notation we use throughout this paper appears in Table 1. For simplicity, we refer to the similarity testing server as the server.

Formalizing SBB. We formalize embeddings first. A similarity embedding method is a function $\mathcal{F}\colon \mathcal{W} \to \{0,1\}^\ell$ for the space of images $\mathcal{W}$ and where ℓ is a parameterizable length. Some embeddings map images to $\mathbb{R}^\ell$ (or a suitably granular approximation of it), but we focus on bit strings unless explicitly mentioned otherwise. Associated with $\mathcal{F}$ is a distance measure $\Delta\colon \{0,1\}^\ell \times \{0,1\}^\ell \to \mathbb{Z}$. We focus on Δ being Hamming distance. Most often one sets an application-dependent threshold T as the definition of similarity, and builds $\mathcal{F}$ so that matches with distance values smaller than T indicate the images depicted are perceptually similar.

An example $\mathcal{F}$ is the aforementioned PDQHash [1]. PDQHash was designed to capture the "syntactic" similarity between images. Syntactic similarity captures if two images are essentially the same, e.g., the same image but of different quality, or rotated slightly. This is different from semantic similarity, which focuses on whether images share the same features, e.g., the same person. Algorithms designed for syntactic similarity also include PhotoDNA [51] and pHash [78]. PDQHash first converts a given image w from RGB to luminance, then uses two-pass Jarosz filters to compute a weighted average of 64×64 subblocks of the luminance image. Given the 64×64 downsample, the algorithm computes a two-dimenstional discrete cosine transform (DCT), and keeps only the first 16 slots in both X and Y directions. After that, each entry of the 16×16 DCT output is transformed into a binary bit after being compared to the median, with 1 indicating larger than the median and 0 indicating otherwise.

Symbol	Description
w / $\mathcal{W}$	an image / set of all images
$\mathcal{B}$	set of images held by server
$\mathcal{D}$	distribution from which images are sampled
ℓ	length of similarity embedding
$\mathcal{F}$	similarity embedding method
v / $\mathcal{Y}$	result of similarity embedding / set of all such results
Δ	distance function between two similarity embeddings
T	distance threshold for similarity matching using Δ
$\mathcal{D}_\mathcal{F}$	distribution of similarity embeddings induced by $\mathcal{F}$
Emb	coarse embedding algorithm
Sim	coarse embedding similarity algorithm
p	an output of Emb
d	length of p
B	candidate bucket generated from Sim
γ	parameter of $\mathbb{E}_{LSH}$, flipping bias
k	coarse threshold of Sim

Table 1: Notation frequently used in this paper.

Coarse embedding schemes. To allow bucketization via similarity, we define a coarse embedding scheme $\mathbb{E} = (\mathrm{Emb}, \mathrm{Sim}, (\mathcal{W}, \Delta_\mathcal{W}))$, as a pair of algorithms and an associated metric space. The (possibly randomized) embedding algorithm $\mathrm{Emb}(w)$ takes as input a value $w \in \mathcal{W}$ and outputs a value $p \in \{0,1\}^d$. Here d is a configurable parameter. We call p the embedding of w, or simply the embedding when w is clear from context. The deterministic algorithm $\mathrm{Sim}(p, w')$ takes as input $p \in \{0,1\}^d$ and $w' \in \mathcal{W}$ and outputs a bit. The bit being one indicates that the embedding of w' is similar to the embedding of w, which is denoted as p. It will be convenient to abuse notation, by letting $\mathrm{Sim}(p, \mathcal{B})$ be defined to output the set $\{w' \mid w' \in \mathcal{B} \wedge \mathrm{Sim}(p, w') = 1\}$.

One idea for a coarse embedding scheme would be to simply use $\mathcal{F}$ directly, but with smaller ℓ and smaller T. To be specific, using PDQHash as an example, a coarse PDQHash scheme $\mathbb{E}_{cPDQ} = (\mathrm{Emb}_{cPDQ}, \mathrm{Sim}_{cPDQ}, (\mathcal{W}, \Delta_\mathcal{W}))$ can be implemented as follows: $\mathrm{Emb}_{cPDQ}(w)$ computes the hash of w on the first 4×4 slots of the DCT output, rather than 16×16 of the output, producing a 16-bit binary string. The 16-bit value can then provide much cruder similarity comparison. Then $\mathrm{Sim}_{cPDQ}(p, \mathcal{B})$ iterates over all $w' \in \mathcal{B}$, hashes them, and returns those with distance smaller than a coarse threshold k as a bucket B. Unfortunately this scheme doesn't meet our privacy goals, as we will explore in detail in Section 5.

Correctness and compression efficiency. We define $\Delta_\mathcal{W}$ via an existing similarity embedding $\mathcal{F}$, i.e., $\Delta_\mathcal{W}(w, w') = \Delta(\mathcal{F}(w), \mathcal{F}(w'))$. We say that a coarse embedding scheme is $(T, \varepsilon, \mathcal{D})$-correct if, for an image w sampled from $\mathcal{D}$, a distribution over $\mathcal{W}$, and for any w' such that $\Delta_\mathcal{W}(w, w') < T$, we have that $\Pr[\mathrm{Sim}(\mathrm{Emb}(w), w') = 1] \geq 1 - \varepsilon$, where the probability is taken over the random coins used by Emb and the choice of w from $\mathcal{D}$. A trivial coarse embedding scheme is to just use $\mathcal{F}$ itself, which would be $(T, 0, \mathcal{D})$-correct for any T and $\mathcal{D}$. But as mentioned, doing this will not provide the desired privacy.

Another type of trivial coarse embedding scheme is to have Sim always output one. Then Emb could output a fixed constant value regardless of input, meaning nothing leaks about w. This would also be $(T, 0, \mathcal{D})$ correct for arbitrary T and any given $\mathcal{D}$, but won't be useful because, in our SBB application, the bucket would end up being the entire set $\mathcal{B}$.

We define a compression efficiency metric as follows. A coarse embedding scheme is $(\mathcal{B}, \alpha, \mathcal{D})$-compressing if for a distribution $\mathcal{D}$ over $\mathcal{W}$, $\mathcal{B} \subseteq \mathcal{W}$, w drawn from $\mathcal{D}$ we have that $\mathrm{E}\left[\frac{|B|}{|\mathcal{B}|}\right] \leq \alpha$ where $B = \{w' \mid w' \in \mathcal{B}, \mathrm{Sim}(\mathrm{Emb}(w), w') = 1\}$ and the probability space is over the choice of w from $\mathcal{D}$ and the coins used by Emb. This measures the average ratio of bucket size to dataset size.

LSH-based coarse embedding. We propose a coarse embedding scheme that is based on locality sensitive hashing (LSH) [29]. An LSH function family allows approximate nearest neighbour search with high-dimensional data. Formally, the scheme $\mathbb{E}_{LSH} = (\mathrm{Emb}_{LSH}, \mathrm{Sim}_{LSH}, (\mathcal{W}, \Delta_{\mathcal{W}}))$ is defined as follows (see also Figure 2). Let $\mathcal{I}$ be a family of hash functions that maps points from a high-dimensional input space $\mathbb{I}$ into a hash universe U of lower dimension. When $\mathbb{I} = \{0,1\}^{\ell}$ and Δ is Hamming distance, the construction of an LSH function family is intuitive. For an ℓ-bit string v, we denote the individual bits as $v_1, \ldots, v_{\ell}$. An indexing function is a map $I\colon \{0,1\}^{\ell} \to \{0,1\}$ and we let $\mathcal{I}$ be the set of all index functions, which is the LSH function family.

In our context, we randomize the selection of LSH functions for every individual query, and add noise to ensure privacy. Emb_{LSH} takes an image w as input, and computes the similarity embedding of it via $v \leftarrow \mathcal{F}(w)$. In our implementation, we use PDQHash for $\mathcal{F}$. Our protocol works on other types of embedding functions that use Hamming distance as a metric, such as pHash [78]. We sample d bits from v by sampling d LSH functions without replacement and flip each bit with probability γ. The resulting embedding with added noise and the indices are shared with the server. The server performs Sim_{LSH} by comparing the received bits to the corresponding bits of $\mathcal{F}(w_i)$ for each $w_i \in \mathcal{B}$, adding w_i to the bucket B if sufficiently many of these bits match.

To formalize this, we abuse notation slightly. We denote I as a map $\{0,1\}^{\ell} \to \{0,1\}^{d}$, a combination of d functions sampled uniformly from $\mathcal{I}$ without replacement. Similarly, one can easily encode an indexing function as a set of indexes; we treat I both as a function and its encoding. We let Flip_{γ} be the randomized algorithm that takes as input a bit string p and outputs $\tilde{p}$ of the same length, setting $\tilde{p}_i = p_i$ with probability $1 - \gamma$ and $\tilde{p}_i = \neg p_i$ with probability γ. The full algorithms

$\underline{\mathrm{Emb}_{LSH}(w)}$	$\underline{\mathrm{Sim}_{LSH}((I,p), \mathcal{B})}$
$v \leftarrow \mathcal{F}(w)$	$B \leftarrow \{\}$
$I \leftarrow\!\!\$\ \mathcal{I}$	For $w \in \mathcal{B}$:
$p \leftarrow\!\!\$\ \mathrm{Flip}_{\gamma}(I(v))$	If $\Delta(p, I(\mathcal{F}(w))) \leq k$ then
Return (I, p)	$B \leftarrow B \cup \{w\}$
	Return B

Figure 2: Coarse embedding scheme $\mathbb{E}_{LSH}$.

for $\mathbb{E}_{LSH}$ are shown in Figure 2. We use a threshold k for the Hamming distance over the randomly selected indexes. We formally analyze correctness of $\mathbb{E}_{LSH}$ in the extended version [35]. Different choices of the parameter sets of $\mathbb{E}_{LSH}$, i.e., embedding length d, flipping bias γ, and coarse thresholds k result in different combination of privacy loss, correctness, and bucket compression rate. We further explore this trade-off in Section 5.

One limitation of $\mathbb{E}_{LSH}$ arises should an adversary be able to collect many queries that it knows are for the same image. Eventually it will see all bit locations, and even have enough samples to average out the noise (e.g., via a majority vote for each bit location). We discuss this further in Section 7.

Similarity protocols. A coarse embedding scheme will not suffice to perform a full similarity check. Instead, we compose such a scheme to perform SBB with a similarity protocol where the server uses the resulting bucket $B \leftarrow\!\!\$\ \mathrm{Sim}(\mathrm{Emb}(w), \mathcal{B})$. The composition achieves privacy levels related to the protocol's for $\mathcal{B}$, and correctness proportional to the product of the coarse embedding and the protocol's correctness. We discuss some examples and their properties here. These examples ensure perfect correctness, hence the correctness of the composition depends solely on that of the coarse embedding. In Section 5.4, we show that for various similarity protocols, both runtime efficiency and bandwidth are largely improved when combined with SBB.

Similarity embedding retrieval. A pragmatic similarity protocol has the server send to the client the similarity embeddings of all the elements in the bucket, i.e., send $v_1, \ldots, v_{|B|}$ where $v_i = \mathcal{F}(w_i)$ for each $w_i \in B$. The client can then compute $\mathcal{F}(w)$ and compare against each v_i. This approach reduces the confidentiality for the server's dataset, since now clients learn all the similarity embeddings in $\mathcal{B}$ that fall into the bucket. It may also reduce resistance to evasion attacks, but in contexts where client privacy is paramount this simple protocol already improves on existing approaches.

Secure-sketch similarity protocol. We can improve server confidentiality via a secure-sketch-based [20] similarity protocol. The protocol ensures that the client can only learn the similarity hashes that are close to a client-known value. If images in the database have sufficiently high min-entropy then the secure sketch ensures that the client cannot learn it. This assumption may not always hold (most obviously in the case that the client has a similar image), in which case confidentiality falls back to that achieved by similarity embedding retrieval. We defer details to the extended version [35].

2PC similarity protocols. Finally, one may compose SBB with an appropriate 2PC for similarity comparisons. Such an approach provides better confidentiality for $\mathcal{B}$, but at the cost of larger bandwidth and execution time. We experiment with two frameworks: CrypTen [41] and EMP [72]. CrypTen is a secret-sharing-based semi-honest MPC framework for Python that is geared toward machine learning applications. CrypTen currently relies on a trusted third party for certain operations, including generating Beaver multiplication triples [9]. Generation of Beaver triples using Pailler [56] is actively under development. EMP is a circuit-garbling-based generic semi-honest 2PC framework that is implemented in C++.

Both frameworks above target semi-honest security. One could also compose SBB with a maliciously secure 2PC protocol, with caveat that a malicious server is not bound to correctly execute the SBB Sim algorithm and so could deviate by adding arbitrary values to the bucket. In our context, such an attack can anyway be performed by just modifying $\mathcal{B}$ in the first place, but this could be relevant in future work, particularly as it relates to accountability mechanisms that monitor for changes to $\mathcal{B}$.

4 Privacy of Coarse Embeddings

In this section, we detail our framework for reasoning about privacy threats against coarse embeddings. Our framework is designed to analyze the adversary's confidence in assessing a predicate being true or not, when given one or multiple client requests as input. Here we only consider client privacy; privacy of the server's dataset can be achieved by composing SBB with a suitable similarity protocol (see Section 3).

Proposed security measures. We consider settings where an adversary receives the embedding(s) of one or more images, and wants to infer some predicate over the images. Let $\mathcal{W}^q$ be the Cartesian product of q copies of $\mathcal{W}$. We denote tuples of images in bold, $\mathbf{w} \in \mathcal{W}^q$ and $\mathbf{w}[i] \in \mathcal{W}$ for $i \in [1,q]$. Let Emb($\mathbf{w}$) be the result of running Emb independently on each component of $\mathbf{w}$, denoted as $\mathbf{p}$. That is, $\mathbf{p} \leftarrow\!\!\$\ \mathrm{Emb}(\mathbf{w})$ is shorthand for $\mathbf{p}[i] \leftarrow\!\!\$\ \mathrm{Emb}(\mathbf{w}[i])$ for $i \in [1,q]$.

To start, consider a distribution $\mathcal{D}$ over $\mathcal{W}^q$ and a predicate $f\colon \mathcal{W}^q \to \{\mathsf{false}, \mathsf{true}\}$. We want to understand the ability of an adversary to infer $f(\mathbf{w})$ when given Emb($\mathbf{w}$) for $\mathbf{w}$ drawn from $\mathcal{W}^q$ according to $\mathcal{D}$. As an example, let $q = 1$ and have f indicate whether a client image has the same perceptual hash value with that of another image that is chosen by the adversary. We'd like to have a guarantee that revealing Emb($\mathbf{w}$) doesn't allow inferring that the images are similar with high confidence. We refer to a tuple $\pi = (\mathcal{D}, \mathcal{W}^q, f)$ as a privacy setting.

We provide three measures of adversarial success: accuracy, precision, and area under the receiver-operator curve

$\mathrm{PRED}_{\mathrm{Emb},\pi}$
$\mathbf{w} \leftarrow_{\mathcal{D}} \mathcal{W}^q$
$p \leftarrow\!\!\$\ \mathrm{Emb}(w)$
$b \leftarrow\!\!\$\ \mathcal{A}(p)$
Return $(b = f(\mathbf{w}))$

$\mathrm{AUC}_{\mathrm{Emb},\mathcal{D}}$
for $i \in \{\mathsf{true}, \mathsf{false}\}$
$\quad \mathbf{w}_i \leftarrow_{\mathcal{D}_i} \mathcal{W}^q$
$\quad \mathbf{p}_i \leftarrow\!\!\$\ \mathrm{Emb}(\mathbf{w}_i)$
$\quad r_i \leftarrow\!\!\$\ \mathcal{A}_{\mathrm{auc}}(\mathbf{p}_i)$
Return $r_{\mathsf{true}} > r_{\mathsf{false}}$

Figure 3: Pseudocode games for measuring embedding privacy. Here f represents a predicate.

(AUC), thereby adapting traditional measures of efficacy for prediction tasks to our adversarial setting.

Accuracy. Let $\mathcal{A}_{\mathrm{acc}}$ be a randomized algorithm, called an accuracy adversary. We define a probabilistic experiment that tasks $\mathcal{A}$ with inferring $f(\mathbf{w})$ given Emb($\mathbf{w}$) for $\mathbf{w}$ drawn according to $\mathcal{D}$. This probability space is over the coins used to sample $\mathbf{w}$, to run Emb a total of q times, and to run $\mathcal{A}_{\mathrm{acc}}$. We let "$\mathcal{A}_{\mathrm{acc}}(\mathrm{Emb}(\mathbf{w})) = f(\mathbf{w})$" be the event that $\mathcal{A}_{\mathrm{acc}}$ outputs the correct value of the predicate. We write this as a pseudocode game $\mathrm{PRED}_{\mathbb{E},\pi}$ shown in Figure 3, where the returned value captures the event that $\mathcal{A}$ succeeds. For skewed distributions, the trivial adversary that ignores its input and simply predicts the most likely predicate value may achieve high accuracy. We therefore define the advantage of $\mathcal{A}_{\mathrm{acc}}$ as the improvement over that trivial approach:

$$\varepsilon_{\mathrm{acc}} = \frac{\Pr\left[\mathcal{A}_{\mathrm{acc}}(\mathrm{Emb}(\mathbf{w})) = f(\mathbf{w})\right] - \varepsilon_{base}}{1 - \varepsilon_{base}} ,$$

where $\varepsilon_{base} = max(\Pr\left[f(\mathbf{w}) = 1\right], \Pr\left[f(\mathbf{w}) = 0\right])$.

Precision. For adversaries that are mainly interested in inferring positive instances, $f(\mathbf{w}) = \mathsf{true}$, accuracy may appear misleading in cases with high skew, i.e., when $f(\mathbf{w}) = \mathsf{false}$ happens almost always [47]. In our running example, we expect that in practice most images handled by clients will be distinct from the adversary-chosen one.

We therefore also provide two other security measures. First, we measure the precision of a non-trivial adversary in inferring $f(\mathbf{w})$. By non-trivial, we mean that the adversary has to predict $f(\mathbf{w}) = \mathsf{true}$ at least once. We use the same probability space as in the previous definition. To emphasize that the best adversary for achieving high precision may differ from the best one for maximizing accuracy improvement, we use $\mathcal{A}_{\mathrm{pre}}$ to denote the adversary when considering precision. We want to measure the probability that $\mathcal{A}_{\mathrm{pre}}$ succeeds, conditioned on $\mathcal{A}_{\mathrm{pre}}$ outputting true. We denote this by $\Pr\left[f(\mathbf{w}) = \mathsf{true} \mid \mathcal{A}_{\mathrm{pre}}(\mathrm{Emb}(\mathbf{w})) = \mathsf{true}\right]$. To prevent $\mathcal{A}_{\mathrm{pre}}$ from using the trivial strategy of predicting all events as negative, we define an affiliate concept of recall r as

$$r = \Pr\left[\mathcal{A}_{\mathrm{pre}}(\mathrm{Emb}(\mathbf{w})) = \mathsf{true} \mid f(\mathbf{w}) = \mathsf{true}\right] .$$

We will restrict attention to adversaries $\mathcal{A}_{\mathrm{pre}}$ for which r exceeds some threshold, e.g., $r > 0\%$. We let

$$\varepsilon_{prec}^{r>\rho} = \Pr\left[f(\mathbf{w}) = \mathsf{true} \mid \mathcal{A}_{\mathrm{pre}}(\mathrm{Emb}(\mathbf{w})) = \mathsf{true}\right]$$

denote the precision advantage for some adversary $\mathcal{A}_{\mathrm{pre}}$ that achieves $r > \rho$, with the exception of $\rho = 100\%$, where the restriction is set as $r = 100\%$.

AUC. Precision captures the adversary's confidence in predicting the positive class, i.e., the likelihood of $f(\mathbf{w})$ being true when the adversary predicts it to be true. However, it does not capture the adversary's confidence regarding predicting the negative class. We therefore finally formalize a notion of AUC, where recall that AUC is the area under the receiver-operator curve, a popular measure of classifier efficacy. At a high level, AUC-ROC indicates the classifier's capability in differentiating positive classes from negative ones. For a setting $\pi = (\mathcal{D}, \mathcal{B}^q, f)$, let $\mathcal{D}_i$ be the distribution $\mathcal{D}$ over $\mathcal{W}^q$ conditioned on $f(\mathbf{w}) = i$ for $i \in \{\mathsf{true}, \mathsf{false}\}$. Then for an adversary $\mathcal{A}_{\text{auc}}$ that outputs a real value in $[0,1]$ we measure the probability that $\mathcal{A}_{\text{auc}}(\text{Emb}(\mathbf{w}_{\mathsf{true}})) > \mathcal{A}_{\text{auc}}(\text{Emb}(\mathbf{w}_{\mathsf{false}}))$ where $\mathbf{w}_i$ is drawn from $\mathcal{B}^q$ according to $\mathcal{D}_i$. The probability is over the independent choices of $\mathbf{w}_{\mathsf{true}}$ and $\mathbf{w}_{\mathsf{false}}$, as well as the coins used by the $2q$ executions of Emb and two executions of $\mathcal{A}_{\text{auc}}$. We provide a pseudocode game $\text{AUC}_{\text{Emb},\pi}$ describing this probability space in Figure 3. Then we define the advantage of an AUC adversary $\mathcal{A}_{\text{auc}}$ by

$$\varepsilon_{\text{auc}} = 2 \cdot \Pr\left[\mathcal{A}_{\text{auc}}(\text{Emb}(\mathbf{w}_{\mathsf{true}})) > \mathcal{A}_{\text{auc}}(\text{Emb}(\mathbf{w}_{\mathsf{false}}))\right] - 1 \ .$$

This formulation uses a well-known fact [4, 17] about AUC that it is equal to the probability that a scoring algorithm (in our case, the adversary) ranks positive-class instances higher than negative-class instances. For simplicity, we ignore ties ($\mathcal{A}_{\text{auc}}$ outputting the same value in each case). Without loss of generality, we can assume that the AUC adversary $\mathcal{A}_{\text{auc}}$ wins the game with probability greater than or equal to 0.5, and so the normalization maps to the range $[0,1]$. (This corresponds to the classic Gini coefficient.)

Possible predicates. We focus on the matching predicate in our analyses. An adversary chooses an image w_{adv}, and wishes to determine if the client request $\text{Emb}(w_c)$ corresponds to an image that is very similar to w_{adv}, i.e., $\mathcal{F}(w_c) = \mathcal{F}(w_{adv})$. Had the adversary the confidence to assert that there's a match, they can recover the content from the submitted request. Such an attack is trivial in hashing-based similarity testing services, when the clients are required to submit similarity hashes as their requests. That said, our framework can be used to analyse other predicates. For example, an adversary may want to infer if q different client requests all correspond to similar content. We leave such analyses to future work.

Discussion. We have omitted placing computational limits on adversaries, which would be useful in cases where embedding schemes rely on cryptographic tools — our mechanisms do not. A computational treatment is a straightforward extension to our framework. The security games underlying our measures are conservative, and in particular we assume that the adversary has perfect knowledge of the distribution $\mathcal{D}$ as well as $\mathcal{D}$'s support, which is unlikely in practice. While we do not explicitly model side information that an adversary might have about a client's image, it is possible to include it indirectly in this framework, for example, by changing the distribution or modifying the privacy predicate.

Bayes optimal adversaries. To allow simulations that evaluate privacy, we focus on adversaries that maximize advantage. Recall that we assume that the adversary knows the distribution $\mathcal{D}$ from which the clients are sampling images for their requests. Upon receiving client submitted requests $\mathbf{p} = \text{Emb}(\mathbf{w})$, the Bayes optimal adversary computes the **exact** likelihood of the predicate being true — $\Pr[f(\mathbf{w}) = \mathsf{true} \mid \text{Emb}(\mathbf{w}) = \mathbf{p}]$, probabilities are over the choice of $\mathbf{w}$ being sampled from $\mathcal{W}^q$ and coins used by the executions of Emb.

The Bayes optimal adversary for the precision metric, $\mathcal{A}_{\text{pre}}$, chooses a threshold T_{adv}, such that $\mathcal{A}_{\text{pre}}(\mathbf{w}) = \mathsf{true}$ if and only if $\Pr[f(\mathbf{w}) = \mathsf{true} \mid \text{Emb}(\mathbf{w}) = \mathbf{p}] > T_{adv}$. The adversary may choose T_{adv} to maximize $\varepsilon^{r>\rho}_{prec}$. A similar strategy can be used by $\mathcal{A}_{\text{acc}}$. However when $f(\mathbf{w}) = \mathsf{true}$ is especially rare, the adversary may achieve larger ε_{acc} by predicting all predicates using the majority class, $f(\mathbf{w}) = \mathsf{false}$. When doing so, the optimal ε_{acc} is zero. Note that in our simulations we consider all possible threshold values for the sampled dataset, and report on the one that provides the best success rate. A real attacker would have to pick a threshold a priori, meaning our analyses are conservative.

The Bayes optimal adversary for $\mathcal{A}_{\text{auc}}$ doesn't have to choose a threshold T_{adv}. The adversary is given two scenarios to rank: $\mathbf{w}_{\mathsf{true}}$ and $\mathbf{w}_{\mathsf{false}}$, one has $f(\mathbf{w}_{\mathsf{true}}) = \mathsf{true}$ and the other has $f(\mathbf{w}_{\mathsf{false}}) = \mathsf{false}$. The adversary wins the game when they correctly rank the true scenario over the false one, i.e., when $\mathcal{A}_{\text{auc}}(\mathbf{p}_{\mathsf{true}}) > \mathcal{A}_{\text{auc}}(\mathbf{p}_{\mathsf{false}})$. As $\text{Emb}(\mathbf{p})$ is the only information that the adversary gained from our SBB protocol, the optimal strategy to utilize the information is hence to use $\Pr[f(\mathbf{w}) = \mathsf{true} \mid \text{Emb}(\mathbf{w}) = \mathbf{p}]$ as $\mathcal{A}_{\text{auc}}(\mathbf{p})$.

5 Balancing Security, Correctness, Efficiency

In this section, we demonstrate how to balance security, correctness and compression efficiency of SBB when using the LSH-based coarse embedding scheme $\mathbb{E}_{LSH}$. We do so via simulations using real-world image sharing data collected from social media sites. Using our framework, we evaluate the security of $\mathbb{E}_{LSH}$ with varying parameter settings. We then fix the security requirement and explore the trade-off between correctness and compression efficiency.

5.1 Experimental Setup

Data collection. Recall that our deployment scenario in Section 2, an ideal dataset should represent the image sharing behaviors among users on an end-to-end encrypted messaging platform. However, data of one-to-one shares among users on any private messaging platform is by definition, private.

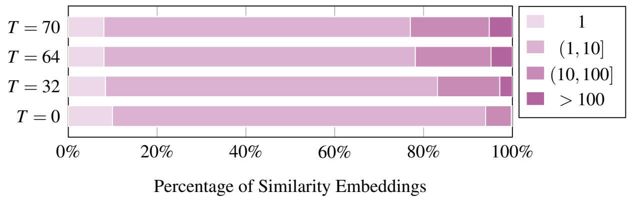

Figure 4: T-Neighborhood size distribution for different T.

Hence, we sought a public dataset that may act as a stand-in for our experiments. As the dataset is publicly available, our experiment did not require review from our IRB office. On Twitter, users may retweet the content that they want to share with their audience. We consider retweets on public Twitter as a proxy for user sharing in private social network. Furthermore, the problem of misinformation, which motivated our study, is prevalent on Twitter [33].

We were able to use a dataset from previous work [34, 36] that contains Twitter interactions with a group of US political candidate accounts between September 13, 2018 and January 6, 2019. The dataset includes 1,190,355 tweets with image URLs, however, by the time of downloading images, only 485 K images were successfully retrieved. We encode the retrieved images with PDQHash. There are 256,049 unique PDQHash values in total. We collect the total number of retweets of each tweet in November 2019: the data was available for 13% of the tweets. The total number of postings and retweets of the images we retrieved adds up to 1.2 million. We simulate a workload for similarity testing as follows. Any tweet and retweet with a valid image is considered as a client request to our system. Hence, this experimental set has 1.2 million client requests with 256 K unique PDQHash values.

Dataset statistics. Users on social media share similar images frequently. The T-neighborhood size of an image w is the number of images that are T-similar to it. Two images are T-similar if and only if their similarity embeddings have a Hamming distance smaller than T. We choose the values of T according to the recommendations from the white paper on PDQHash [1], where 32 and 70 were specified as the lower and upper bounds of recommended similarity thresholds. We also include $T = 0$ and $T = 64$ for comparison.

Figure 4 shows the distribution of T-neighborhood sizes (shades of color) of the images in client requests, with different T (in different rows). The lightest shades (left) are requests with neighborhood size of one, i.e., the neighborhood only contains the single image. The following darker shades are the images with neighborhood size in the range $(1,10]$, $(1,100]$, and $(100,\infty)$. The bottom row shows the neighborhood size distribution with $T = 0$. In our dataset, most of the images in the client requests (84%) share the same similarity embedding with more than one, but fewer than 10 neighbors. The distributions of neighborhood size are mostly similar to each other, especially for $T = 64$ and $T = 70$. Naturally, with a larger threshold, there are more requests containing images with a larger neighborhood size. For example, only 2.85% of all request images have a neighborhood size larger than 100 with $T = 32$ (third row from top, darkest column with purple), while 5.23% of the requests satisfy the same condition when $T = 70$ (first row from top, darkest column with purple).

Implementation. We compare the privacy of SBB when using $\mathbb{E}_{LSH}$ with different embedding lengths d to the baseline method $\mathbb{E}_{cPDQ}$. We focus on the security guarantees against the matching attack and explain our implementation details.

We formally define the matching attack as $\pi^{w_{adv}}_{match} = (\mathcal{D}, \mathcal{W}, f^{w_{adv}}_{match})$, where $\mathcal{D}$ is the distribution over $\mathcal{W}$ that the client requests are sampled from and w_{adv} is an image chosen by the adversary. For any client submitted request with an image w, the adversary wishes to learn the value of $f^{w_{adv}}_{match}(w)$. We have $f^{w_{adv}}_{match}(w) = \texttt{true}$ if and only if the corresponding PDQHash of the two images are the same, i.e., $\mathcal{F}(w) = \mathcal{F}(w_{adv})$. When trying to match the client image to w_{adv}, an adversary who receives the client request through a bucketization protocol is able to filter out images that are not in the bucket. When the client image is in fact similar to w_{adv}, it should most likely be included in the same bucket by definition of correctness. In this case, a w_{adv} whose similarity hash value is shared more frequently than any other image in the same bucket may boost the adversary's confidence in asserting that the client image is a similar match. Hence, having an image with a more popular hash value as w_{adv} increases the adversarial advantage. In the following experiments, we use the image that has the most popular $\mathcal{F}(w)$ as w_{adv}. The same similarity hash appeared in 0.2% of all requests.

To evaluate the privacy guarantees provided by $\mathbb{E}_{LSH}$ and $\mathbb{E}_{cPDQ}$, we iterate over all requests in our dataset and simulate the client, server, and adversary behavior, to compute the security metrics ε_{acc}, ε_{auc}, and $\varepsilon^{cond}_{prec}$.

Coarse PDQHash embedding scheme ($\mathbb{E}_{cPDQ}$). Recall the algorithm of $\mathbb{E}_{cPDQ}$ described in Section 3. The embedding algorithm Emb_{cPDQ} takes an image w as an input, and follows the PDQHash algorithm but with modified parameter settings, to generate a 16-bit coarse PDQHash. This allows coarse grained similarity comparison. When receiving a request $p = \text{Emb}(w)$, the Bayes optimal adversary follows the strategy as described in Section 4. To be specific, the adversary computes the likelihood of the predicate being true, $\Pr[\mathcal{F}(w) = \mathcal{F}(w_{adv}) \mid \text{Emb}_{cPDQ}(w) = p]$, and makes a binary prediction based on the computed likelihood.

LSH-based embedding scheme ($\mathbb{E}_{LSH}$). Recall that in Figure 2, the LSH-based embedding scheme $\mathbb{E}_{LSH}$ consists of two algorithms Emb_{LSH} and Sim_{LSH}. Emb_{LSH} takes an image w as an input, and outputs the selected indexing function and the resulting coarse embedding. To be specific, $\text{Emb}_{LSH}(w)$ randomly selects a length d indexing function I from $\mathcal{I}$, and computes $\tilde{p} = \text{Flip}_\gamma(I(\mathcal{F}(w)))$. The function is parameterized by two parameters: the length of the indexing function d and the bias γ to flip an index that was chosen.

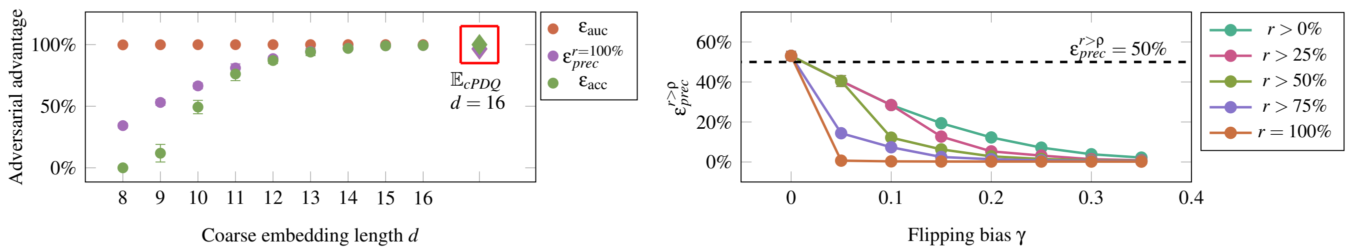

Figure 5: **Left**: Simulation results of the three security metrics, evaluated on (1) $\mathbb{E}_{LSH}$ with embedding length d from 8 to 16 (round markers), $\gamma = 0$ and (2) $\mathbb{E}_{cPDQ}$ (diamond markers in red box). **Right**: The conditioned precision metric $\varepsilon_{prec}^{r>\rho}$ of matching attack, at different recall threshold, with $d = 9$ and varying γ. Error bars in both plots represent the 95% confidence interval.

Note that d is also the length of the coarse embedding. Sim_{LSH} takes the output from Emb_{LSH} and a dataset $\mathcal{B}$ as input, and outputs a candidate bucket as an output. The function has one parameter k, a coarse threshold to choose items for the candidate bucket.

We analyse the security guarantee of $\mathbb{E}_{LSH}$ against the Bayes optimal adversary under the setting of a matching attack $\pi_{match}^{w_{adv}}$. When receiving a request p, as in $p = \mathrm{Emb}(w)$, the Bayes optimal adversary wants to predict $f_{match}^{w_{adv}}(w) = \mathsf{true}$. The adversary bases their prediction on $\Pr[\mathcal{F}(w) = \mathcal{F}(w_{adv}) \mid \mathrm{Emb}_{LSH}(w) = p]$, and computes the probability by using all the information that is revealed to them: the indexing function I, the resulting coarse embedding $\tilde{p}$ and the added noise γ. We define the distribution $\mathcal{D}_{\mathcal{F}}$ of similarity hashes of images sampled from $\mathcal{D}$ as follows: $\mathcal{D}_{\mathcal{F}}(x) = \Pr[\mathcal{F}(w) = x] = \sum_{w' \in \mathcal{W}, \mathcal{F}(w') = x} \mathcal{D}(w')$.

Theorem 1. *Let $\Delta_I(v, p) = \Delta(I(v), p)$ for a similarity hash $v \in \{0,1\}^{\ell}$. Consider a fixed image $w_{adv} \in \mathcal{W}$ and a sampled image $w \leftarrow\!\!\$\, \mathcal{D}$. Let $v_{adv} = \mathcal{F}(w_{adv})$ and $v = \mathcal{F}(w)$. Then*

$$\begin{aligned} &\Pr[v = v_{adv} \mid \mathrm{Emb}(w) = (I, p)] \\ &\quad = \frac{\gamma^{\Delta_I(v_{adv}, p)} \cdot (1-\gamma)^{d - \Delta_I(v_{adv}, p)} \cdot \mathcal{D}_{\mathcal{F}}(v_{adv})}{\sum_{v' \in \{0,1\}^{\ell}} \gamma^{\Delta_I(v', p)} \cdot (1-\gamma)^{d - \Delta_I(v', p)} \cdot \mathcal{D}_{\mathcal{F}}(v')}, \end{aligned}$$

where the probability is over the coins used by Emb *and the choice of w sampled from $\mathcal{D}$.*

We prove this theorem in the extended version [35]. When analysing the security guarantee of $\mathbb{E}_{LSH}$, we vary the parameter settings of d and γ only, as k has no impact on the adversarial advantage. For any choice of d and γ, we randomly choose an index function I, and then execute the protocol for all requests in the dataset. We fix I in the simulation because this information is revealed to the adversary and the adversary computes the likelihood conditioned on the indexing function. We first repeat this process for at least 10 times. For parameter settings that result in large fluctuation in the results, we repeat for another 10 iterations. We were able to obtain a stable estimate for all experiments after at most 20 iterations.

5.2 Privacy of SBB

Using different security metrics. To obtain a broad understanding of the information leakage from our protocol, we present all three security metrics $\varepsilon_{\mathrm{auc}}$, $\varepsilon_{prec}^{r>\rho}$, and $\varepsilon_{\mathrm{acc}}$ in Figure 5 (left). To be specific, we show the results of using (1) $\mathbb{E}_{LSH}$ without added noise (i.e., $\gamma = 0$), but with varying embedding length d, and (2) $\mathbb{E}_{cPDQ}$, a baseline method that embeds a client request into a 16-bit coarse PDQHash. The Y axis denotes the value of the security metrics, ranging from 0 to 100%. The X axis denotes different methods used. From left to right, we list $\mathbb{E}_{LSH}$ with d ranging from 8 to 16 (with round markers). In the red box, to the very right, the diamond markers represent the security metrics for $\mathbb{E}_{cPDQ}$. A naive baseline of using the plaintext similarity embedding (as mentioned in Section 2) achieves 100% for all security metrics (not included in figure).

In our setting, accuracy measures the adversary's performance in predicting the correct class; precision measures the adversary's confidence in predicting the positive class; AUC measures the adversary's ability in differentiating negative classes from positive ones. Our dataset is highly skewed, with more negative predicates than positive ones: only 0.2% of all requests trigger positive matches. This property may lead to a biased view when measured by certain metrics.

Accuracy. In datasets with a skewed distribution, a trivial algorithm that always outputs the majority class, i.e., $f_{match}^{w_{adv}}(w) = \mathsf{false}$, may achieve higher accuracy than any meaningful algorithm that tries to differentiate positive cases from negative cases. In fact, in some cases, when experimenting with $\mathbb{E}_{LSH}$ with $d = 8$, we have $\varepsilon_{\mathrm{acc}} = 0$ (Figure 5 on the left, green markers). This indicates that the adversarial advantage as measured by $\varepsilon_{\mathrm{acc}}$ was based on the performance of the trivial algorithm, hence was considered as none. Meanwhile, other metrics ($\varepsilon_{\mathrm{auc}}$ and $\varepsilon_{prec}^{r=100\%}$) show that the adversarial advantage is non-zero, e.g., $\varepsilon_{prec}^{r=100\%} = 37\%$ for $d = 8$. Both $\mathbb{E}_{cPDQ}$ and $\mathbb{E}_{LSH}$ allow the adversary to have perfect accuracy improvement when performing the matching attack when of similar coarse embedding length. However, applying $\mathbb{E}_{LSH}$ with a smaller coarse embedding length, e.g., $d = 10$ decreases the accuracy improvement to 45%.

Precision. When there's no noise added in $\mathbb{E}_{LSH}$ ($\gamma = 0$), $\varepsilon_{prec}^{r>\rho}$ remains the same regardless of varying recall threshold ρ. We will expand on this point later. With the same value of precision, a larger recall specifies more true positive predicates that the adversary may correctly classify with high confidence, hence larger privacy damage. When using $\mathbb{E}_{LSH}$, decreasing the length of coarse embeddings ($d < 12$) decreases adversarial precision, improving security. However, with embeddings of similar length, $\mathbb{E}_{LSH}$ and $\mathbb{E}_{cPDQ}$ both behave poorly ($d = 15, 16$ compared with $\mathbb{E}_{cPDQ}$).

AUC. Regardless of the embedding schemes, ε_{auc} is almost 100%. The reason is that there are disproportionally many images for which the predicate evaluates as negative that can be easily differentiated from positive ones. Hence, most images with different PDQHashes from w_{adv} are assigned to different buckets than w_{adv}. Therefore, when measured by the adversary confidence of differentiating negative cases from positive ones, as most of the negative cases can be distinguished correctly, the embedding schemes behave poorly. Note that the definition of AUC is in direct conflict with the utility of an SBB scheme, which allows efficiently ruling out images that are not similar with a given client input.

None of the metrics ensures a lower bound for another. While testing on all metrics of adversarial advantage offers a better understanding, it is more practical to focus on a specific security metric that suits the application context. We focus on increasing the adversary's uncertainty in classifying a positive match. This aligns with previous work in the machine learning community that recommends the precision-recall metric over both AUC and accuracy, when evaluating prediction algorithms on highly imbalanced datasets, especially when correctly predicting the positive class is valued more [19, 47, 58, 65]. Hence, $\varepsilon_{prec}^{r>\rho}$ fits our purpose the best, and we focus on it in the following discussion.

Adding noise. We now evaluate the security of $\mathbb{E}_{LSH}$ with added noise, i.e., have $\gamma > 0$. We fix the value of d with $d = 9$ and present results for $\varepsilon_{prec}^{r>\rho}$ in Figure 5 (right) with different values of ρ. The results are similar for other values of d, though the exact value of $\varepsilon_{prec}^{r>\rho}$ differs. The Y-axis denotes $\varepsilon_{prec}^{r>\rho}$ and the X-axis denotes increasing value of γ.

Precision metrics conditioned with different recall thresholds have different meanings. For example, there are 2,533 requests in total that contain images similar to w_{adv}. The metric $\varepsilon_{prec}^{r>0\%}$ measures the confidence of the adversary catching one true positive case out of all, while $\varepsilon_{prec}^{r=100\%}$ measures the confidence of the adversary classifying all 2,533 cases correctly. Naturally we have $\varepsilon_{prec}^{r>0\%} \geq \varepsilon_{prec}^{r=100\%}$. On the other hand, $\varepsilon_{prec}^{r=100\%}$ indicates more advantage for the adversary when having the same value as $\varepsilon_{prec}^{r>0\%}$. When no noise is added ($\gamma = 0$), the adversary computes the same likelihood for all true positive cases when following the strategy as described in Section 4. Hence $\varepsilon_{prec}^{r>\rho}$ remains the same regardless of the recall threshold r. With increasing $\gamma > 0$, it gets harder for the adversary to have high precision while maintaining large recall (green, purple and orange lines).

Even a small value for γ improves the privacy of the client request. For example, when $\gamma = 0.05$ and $d = 9$, the likelihood that at least one value in a client request gets changed is $1-(1-\gamma)^d = 37\%$. That means that in the majority of queries, none of the client request bits will be flipped, nevertheless the possibility that they could have been affects adversarial precision. For example, this results in a drop from 53% (leftmost orange node in Figure 5, right chart) to 40% (second green node from left) for $\varepsilon_{prec}^{r>\rho}$ for $\rho \leq 50\%$. There's a more drastic drop when ρ is larger. When the adversary has to identify more than 50% of the true positives, they have to lower the threshold T_{adv} in predicting a positive answer, this leads to a larger likelihood of being impacted from the uncertainty introduced by the flipping bias. Nevertheless, when having $\gamma \geq 0.05$, $\varepsilon_{prec}^{r>\rho}$ is smaller than 50% (noted by the horizontal line) for all recall thresholds. This indicates that for any given query that the $\mathcal{A}_{\text{pre}}$ predicts as `true`, the adversarial success rate is lower than randomly flipping a coin.

In summary, these results show that using coarse PDQHash $\mathbb{E}_{cPDQ}$ fails to provide privacy for clients. The naive solution of revealing the plaintext similarity embeddings to the server also provides no privacy. Different security metrics demonstrate different aspects of adversarial advantage. We focus on $\varepsilon_{prec}^{r>\rho}$ as its definition fits our privacy goal the best. For our purpose, we consider $\varepsilon_{prec}^{r>0\%} < 50\%$ as our security goal, i.e., when the majority of an adversary's positive guesses (given that there's at least one) are wrong. Given our empirical analysis, we suggest that a reasonable choice of parameters is embedding length $d = 9$ and flipping bias $\gamma = 0.05$, but caution that the privacy performance may vary in practice should the image distribution be very different (see Section 7).

5.3 Correctness and compression efficiency

We show the tradeoff between correctness and bucket compression rate under the security parameters suggested above ($d = 9, \gamma = 0.05$). We vary the value of the coarse threshold k, which specifies the bucket being sent from the server side when performing Sim_{LSH}. Formally, we refer to the notion of correctness as ε in the definition of $(T, \varepsilon, \mathcal{D})$-correct, bucket compression rate as α in that of $(\mathcal{B}, \alpha, \mathcal{D})$-compressing (see Section 3). We use the dataset as $\mathcal{D}$, which we refer to as $\mathcal{D}_{twitter}$ and all the possible values of PDQHash in the dataset as $\mathcal{B}$. We randomly select 2 million requests with replacement and perform the protocol, and take the average value of the correctness and compression rate from all iterations.

In Figure 6, we present the trade-off between correctness and compression efficiency. We plot the correctness ε (Y-axis) as the average compression rate α varies (X-axis). The dashed horizontal line represents 95%. We experiment with different definitions of similarity, i.e., with different values of T, denoted by different colors. Each node represents a pa-

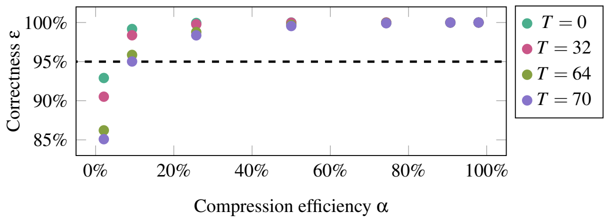

Figure 6: Correctness (with varying similarity threshold T) and compression rate tradeoff. The dashed line marks 95%.

Dataset	Description	Images
IMDB-WIKI [61, 62]	Faces.	523,051
COCO [45]	Common objects.	123,403
T4SA [71]	Twitter images.	1,473,394
Webvision 2.0 [44]	Flickr and Google images.	13,907,566

Table 2: Dataset statistics and description.

rameter setup with the resulting correctness and compression rate. For example, the second blue node from left in Figure 6 represents that with $k = 3$, the resulting embedding scheme is $(32, 98\%, \mathcal{D}_{twitter})$-correct and $(\mathcal{B}, 9.3\%, \mathcal{D}_{twitter})$-compact. Note that our notion of correctness is stricter than the false negative rate defined in the prior work [42] for the Kulshrestha-Mayer protocol, as the prior work measures the rate of transformed images that are not mapped to the original one, constrained on the fact that the PDQHash of the transformed image stays in normalized Hamming distance 0.1 to the original. The protocol [42] reported an average false positive rate of 16.8% on a different dataset. Using our definition, this would be estimated as $(25.6, 83.2\%, \mathcal{D}_{KM})$-correct.

In conclusion, these experiments suggest that for $\mathcal{D}_{twitter}$, one can achieve $\varepsilon_{prec}^{r>0\%} < 50\%$, over 95% correctness for the investigated values of T and 9.3% compression rate using $\mathbb{E}_{LSH}$ with $d = 9$, $\gamma = 0.05$ and $k = 3$. Hence, the resulting scheme achieves an almost order of magnitude reduction in the amount of data input to a second-stage similarity protocol.

5.4 End-to-end Simulation

We now perform end-to-end simulation on varying sizes of blocklists $\mathcal{B}$ to demonstrate the improvement of execution time and bandwidth for different similarity protocols combined with SBB. For the experiments, we use parameters suggested in Section 5.3, i.e. $d = 9$, $\gamma = 0.05$ and $k = 3$.

Datasets. To form varying sizes of blocklist $\mathcal{B}$, we randomly sample images from the datasets that were used in prior work [42].[4] The details of the datasets are listed in Table 2. In particular, for each experiment, we generate $\mathcal{B}$ of the requisite size by uniformly selecting images (without replacement) from the union of the COCO, T4SA, and Webvision 2.0 datasets. For client requests, we sample half of the requests from the IMDB-WIKI dataset to simulate requests that don't match any image in the block list, and the rest from the generated $\mathcal{B}$ to simulate client requests that return a match.

For each set of experiments with a randomly generated $\mathcal{B}$ tested with similarity embedding retrieval (the server simply sends the embeddings of bucket entries to the client), we provide measurements over 40 iterations. With secure sketch, we use 20 iterations and with 2PC protocols, we use 10 iterations because these take significantly longer to run.

Implementation. We use an AWS EC2 p2.xlarge[5] instance with 61 GiB of memory and 200 GiB disk storage for the server side computation. The instance is initialized with the deep learning AMI provided by Amazon. An AWS EC2 t2.small[6] instance with 2 GiB of memory and 64 GiB storage in the same region acted as a client. The measured bandwidth between the two instances was 1 Gbits/sec for both directions and the network latency was 0.9 ms. The server side implementation uses Python and is parallelized using the GPU. The client side implementation uses Go. For the secure sketch protocol, we use an oblivious pseudorandom function (OPRF), implemented by the circl Go library from CloudFlare [27].

For the 2PC protocols our setup is identical except that we use an AWS EC2 t2.large instance with 8 GiB of RAM as the client to be able to handle the 2PC frameworks. The bandwidth was measured to be 1.01 Gbits/sec from server to client, 721 Mbits/sec from client to server. The observed network latency was 0.3 ms. For both the CrypTen and EMP frameworks, we used the computed functionality that checks if there exists a hash among the server's input that has Hamming distance less than T to the client-provided hash. The server's input is the entire $\mathcal{B}$, and the generated SBB bucket, in the non-bucketized and bucketized setting, respectively. We further XOR the output of this comparison with a randomly-generated client-provided bit so that only the client learns the result. For CrypTen, for simplicity we configured the trusted-third party for Beaver triple generation to run on the same EC2 instance as the client (so-called trusted first-party mode). This is not a secure configuration but provides lower bounds on performance (moving Beaver generation to another server would decrease performance). Experimental results for CrypTen should therefore be considered to be lower bounds on performance for secure deployments. Note that our 2PC prototypes are not optimized, and absolute timings would be improved using custom protocols for our setting such as the Kulshrestha-Mayer protocol [42]. However, it is unclear if the protocol can be combined with SBB since it requires generating all buckets at setup time.

Results. We present the average total execution time, average total bandwidth, and the speedup provided by SBB for varying $|\mathcal{B}|$ in Table 3. The execution time and total bandwidth do not vary much between client requests that match images in $\mathcal{B}$ and those that do not. Many of the similarity

[4] These are unfortunately not suitable for the privacy simulations of previous sections; they don't include information about sharing frequency.

[5] https://aws.amazon.com/ec2/instance-types/p2/

[6] https://aws.amazon.com/ec2/instance-types/t2/

$\lvert\mathcal{B}\rvert$	Execution Time (s) No SBB	Execution Time (s) SBB	Total Bandwidth (MiB) No SBB	Total Bandwidth (MiB) SBB	Execution Time (s) No SBB	Execution Time (s) SBB	Total Bandwidth (MiB) No SBB	Total Bandwidth (MiB) SBB
	Similarity Embedding Retrieval				**Secure Sketch**			
2^{18}	0.76 (0.00)	0.02 (0.00)	18.41 (0.00)	0.21 (0.01)	1664.98 (870.78)	2.77 (0.17)	78.81 (0.36)	0.89 (0.05)
2^{19}	1.55 (0.01)	0.03 (0.01)	36.84 (0.02)	0.46 (0.15)	5702.44 (3049.44)	6.03 (0.41)	158.66 (2.39)	1.90 (0.14)
2^{20}	3.09 (0.01)	0.06 (0.02)	73.65 (0.00)	0.83 (0.06)	–	12.09 (0.99)	–	3.56 (0.26)
2^{21}	6.17 (0.01)	0.10 (0.01)	147.31 (0.01)	1.69 (0.12)	–	26.70 (2.40)	–	7.18 (0.55)
2^{22}	12.41 (0.07)	0.43 (0.99)	294.61 (0.03)	3.33 (0.25)	–	61.99 (6.63)	–	14.35 (1.17)
2^{23}	–	0.40 (0.02)	–	6.70 (0.41)	–	157.57 (14.41)	–	28.40 (1.68)
	CrypTen				**EMP**			
2^{13}	17.85 (0.18)	1.18 (0.31)	941.42 (0.37)	11.26 (1.64)	13.14 (0.06)	0.21 (0.01)	1520.63 (0.44)	17.14 (1.82)
2^{14}	36.65 (0.44)	1.33 (0.30)	1882.82 (0.87)	21.40 (2.14)	26.93 (0.98)	0.36 (0.03)	3040.57 (1.39)	34.52 (4.12)
2^{15}	71.76 (0.07)	1.55 (0.06)	3766.55 (0.81)	42.43 (4.06)	54.61 (1.26)	0.67 (0.03)	6079.48 (2.67)	70.45 (3.68)
2^{16}	147.10 (0.66)	2.19 (0.08)	7534.29 (0.90)	83.77 (6.96)	117.52 (8.11)	1.21 (0.14)	12158.00 (0.88)	133.42 (16.20)
2^{17}	–	3.55 (0.40)	–	167.70 (14.69)	–	2.42 (0.13)	–	275.52 (15.32)
2^{18}	–	6.45 (0.40)	–	347.53 (22.65)	–	4.79 (0.28)	–	551.26 (32.51)
2^{19}	–	13.77 (1.22)	–	695.30 (45.49)	–	9.63 (0.52)	–	1097.53 (59.78)
2^{20}	–	27.89 (1.88)	–	1386.84 (107.27)	–	20.24 (1.26)	–	2299.33 (143.63)

Table 3: Average time and bandwidth of similarity protocols without and with SBB for four different similarity testing protocols. Dashes (–) indicate when execution failed due to poor scaling. Numbers in parentheses are standard deviations.

testing protocols do not scale well, and we denote by dashes in the table experiments that failed to complete. Typically this was due to the client instance running out of memory. In all these cases, SBB was able to increase scaling to complete executions with the available resources.

Our results show that SBB drastically improves the similarity protocol's performance, both in terms of execution time and total bandwidth. For similarity embedding retrieval, SBB provides a 29× speedup ($\lvert\mathcal{B}\rvert = 2^{22}$) in execution time. For large-scale datasets ($\lvert\mathcal{B}\rvert \leq 2^{23}$), similarity embedding retrieval with SBB returns the answer in real time, under 0.5 seconds. For the secure sketch protocol, the improvement is even larger, the speedup is at least 601× for $\lvert\mathcal{B}\rvert = 2^{18}$. For 2PC protocols, the improvement provided by SBB grows larger as $\mathcal{B}$ becomes bigger, when $\lvert\mathcal{B}\rvert = 2^{16}$, the speedup in execution time is 67× and 97× for CrypTen and EMP, respectively. For $\lvert\mathcal{B}\rvert = 2^{20}$, EMP with SBB takes less time than the Kulshrestha-Mayer protocol (20.24s vs 27.5s), however it requires larger bandwidth.

6 Related Work

Secure proximity search. Secure proximity search based on general multi-party computation has been used in many applications, including privacy-preserving facial recognition [24, 64], biometric authentication [8, 25], querying sensitive health data [7], and more. However, these works don't scale sufficiently for our use case. More scalable solutions include fuzzy extractors [20, 38], which give a small piece of client information to the server, that does not leak information about the secret, in order to derive secrets from noisy readings such as biometrics. However, the security guarantee is based on the assumption that the distribution of the secret (for example, fingerprints) has enough minimum entropy, which is not necessarily true for image distributions.

Private information retrieval. Chor et al. [14] introduced the concept of private information retrieval, a type of protocol that enables a client to retrieve an item from a database such that the identity of the item is not revealed to the server. The protocol requires clients to supply the index of the data item that they are querying about for retrieval purposes. However, this is unlikely to be applied to our use case. The most likely solution for similarity lookup is content-based privacy preserving retrieval [46, 66, 75]. Previous works [46, 75] in this area assume three parties involved in this type of protocol, a data owner, the client who queries the service and an actual server where the service is hosted. The data owner encodes images or other types of multimedia into feature vectors that are further encoded with searchable encryption schemes and used as indices. The server is made oblivious to the actual content of indices and the content of corresponding data items. The client queries the server by generating indices from their images and receives the data items as answers. The threat model doesn't prevent the case when the data owner colludes with the server, hence cannot be directly applied to our scenario, where the data owner is the server.

Secure k nearest neighbors search. Another possible solution is to use secure k nearest neighbors search (k-NNS) to look for similar items at the server side without revealing client information. Most of the k-NNS solutions require a linear scan of the database that is queried against. Recent work [13] proposed a sub-linear clustering-based algorithm, yet the solution requires significant preprocessing time for each client. Similar to our work, Riazi et al. [60] used locality sensitive hashing to encode client queries for efficient k-NNS. Different from our approach, they preserved user privacy by converting the LSH encodings to secure bits. However, the notion of security is different in their work, in particular, an adversary can estimate the similarity of two given data points based on the encodings. This makes the protocol vulnerable to the matching attack, which we addressed in our work.

Location-based services. We draw comparisons between our bucketization setting and that of location-based services (LBSs). Andrés et al. [6] propose a privacy-preserving mechanism in which mobile clients send their noise-perturbed locations to a server in order to obtain recommendations for nearby restaurants. One may view the noise-perturbed location as a coarse embedding and the server-provided list of restaurants as a similarity bucket. Similar to our coarse embedding scheme, the mechanism of Andrés et al. suffers from privacy loss when applied repeatedly to the same user input. These connections suggest that our framework could have applications to reasoning about LBS privacy. Conversely, insights from location privacy may serve as inspiration for improved SBB mechanisms.

Privacy measures. Prior work has proposed measuring privacy using an adversary's expected error when making inferences based on a posterior distribution on user inputs [55, 67, 68]. Recent work has explored the Bayes security measure [12], which is similar to ε_{acc}, but involves a security game in which the adversary attempts to recover a secret input as opposed to guessing a predicate on the secret input. Local differential privacy [22] has also proven to be a popular worst-case privacy measure, but often incurs high correctness penalties. Although similar, these metrics can not be directly applied to our scenario nor replace ε_{auc} and $\varepsilon_{prec}^{r>\rho}$.

7 Limitations

Our work naturally suffers from several limitations that should be explored further before deployments are considered. Most notably, use of an SBB mechanism fundamentally must leak some information to the server to trade-off client privacy for efficiency. In some contexts leaking even a single bit of information about user content would be detrimental, in which case our techniques are insufficiently private. We speculate that leaking some information about client images is, however, fundamental to achieve practical performance in deployment for large $\mathcal{B}$. How to provide a formal treatment establishing that scaling requires some leakage and what that means for moderation mechanisms remain open questions.

Second, our empirical analyses focus on matching attacks for a single query, which excludes some other potential threats. In particular it does not address adversarially-known correlations between multiple images queried by one or more clients. A simple example, mentioned in Section 3, is an 'averaging' attack against our LSH-based coarse embedding in which the adversary obtains a large number of embeddings all for the same image w. Then the adversary can average out the per-bit noise and recover the granular embedding $\mathcal{F}(w)$. We discuss simulation results for this scenario in the extended version [35]. The results indicate that, similar to privacy-preserving mechanisms for location-based services [6, 12, 55, 67], repeated queries on the same content drastically weaken the privacy guarantee of SBB: an adversary that sees multiple SBB outputs that it knows are for the same image can obtain near-perfect matching attack precision for almost all recall thresholds.

To address risk here, client software might cache images they've recently queried. The client would not query the similarity service if a new image is too close to a prior image, and instead just reuse the cached result for the latter. Caching may not be feasible in all cases, and doesn't speak to cross-user sharing of images, which may be inferrable from traffic analysis should the adversary have access both to the similarity service and the messaging platform. Another approach would be to somehow ensure that the same noise is added to the same image, regardless of which client is sending it. This could possibly be done by having some clients share a secret key, and use it to apply a pseudorandom function to the image (or its PDQHash) to derive the coins needed for the random choices underlying our coarse embedding. Here an adversary's $\varepsilon_{prec}^{r>0\%}$ advantage remains at 50% regardless of the increasing number of repeated queries. But this doesn't account for other potentially adversarially-known correlations across images (e.g., they are almost identical), and may be fragile in the face of malicious client software. Moreover, sending the same SBB embedding for the same image would seem to increase susceptability to linking attacks in which an adversary infers when two or more queries correspond to the same image. We are unsure which scenario bears more risk in practice. We leave the exploration of these mitigations to future work.

A related limitation is the exclusive use of empiricism for evaluation. While we focus on Bayes-optimal adversaries, it would be preferable to couple empiricism with analyses providing bounds on adversarial success. While our definitional framework provides the basis for proving bounds on, e.g., precision for particular data distributions, we do not yet have proofs and it appears to be challenging. We emphasize that such results cannot fully replace empirical work, because even formal results would necessarily make assumptions about data that must be empirically validated. Nevertheless, we consider the empirical results presented in this initial work as a proof-of-concept of the SBB framework and encourage future works to further examine the theoretical bounds for this approach.

Finally, the public perceptual hash algorithms that SBB relies on increases the risk of evasion attacks that seek to modify images just enough to avoid detection. This risk seems particularly acute when using a similarity testing protocol that sends a bucket of PDQHash values to the client, as the adversary could extract these values from a client to inform their attacks. Allowing users to report misinformation images to frequently update the database may mitigate this risk.

8 Conclusion and Future Directions

In this paper, in order to allow efficient privacy-preserving similarity testing, we defined the framework of similarity-based bucketization and formalized a set of privacy goals that are important to this application. We consider the information that the adversary wants to infer from a client input as the answer to a prediction task. An adversary's advantage is measured by their uncertainty regarding the prediction, using metrics that are widely applied in machine learning.

Towards a realistic prototype for SBB, we focus on image similarity testing. Driven by the privacy formalization, we ran simulations on real-world social media data and analyzed the SBB protocol's security against a "matching attack". The attack refers to the scenario where an adversary tries to infer if a client input is similar to an adversary-chosen image. Using our framework, deployments can tune the performance/privacy trade-off depending on the application context. We then test SBB's performance when composed with four similarity protocols with varying server privacy guarantees for the server content. We show that the composition with SBB significantly reduces the protocol latency and required bandwidth. While further research is needed to address various open questions and limitations of our results, we nevertheless believe that SBB represents a promising approach to scaling private similarity testing in practice.

9 Acknowledgements

We thank Lucas Dixon, Nirvan Tyagi, and Paul Grubbs for useful discussions and feedback about this work. We thank Laurens van der Maaten and Brian Knott for answering our questions regarding CrypTen, and Xiao Wang for answering questions about EMP. This research was supported in part by NSF award #1704527.

References

[1] The TMK+PDQF video hashing algorithm and the PDQ image hashing algorithm. Technical report, Facebook, 2019.

[2] Technical solutions to detect child sexual abuse in end-to-end encrypted communications. Technical report, European Commission, 2020.

[3] CSAM detection. Technical report, Apple, 2021.

[4] Shivani Agarwal, Thore Graepel, Ralf Herbrich, Sariel Har-Peled, and Dan Roth. Generalization bounds for the area under the roc curve. *Journal of Machine Learning Research*, 6(Apr):393–425, 2005.

[5] Arooj Ahmed. Whatsapp iOS is testing a search image on the web feature, a clear all messages except starred option and more. *Digital Information World*, 2020.

[6] Miguel E. Andrés, Nicolás E. Bordenabe, Konstantinos Chatzikokolakis, and Catuscia Palamidessi. Geo-indistinguishability: Differential privacy for location-based systems. CCS '13, page 901–914, New York, NY, USA, 2013. Association for Computing Machinery.

[7] Gilad Asharov, Shai Halevi, Yehuda Lindell, and Tal Rabin. Privacy-preserving search of similar patients in genomic data. *Proceedings on Privacy Enhancing Technologies*, 2018(4):104–124, 2018.

[8] Mauro Barni et al. Privacy-preserving fingercode authentication. In *Proceedings of the 12th ACM workshop on Multimedia and Security*, pages 231–240, 2010.

[9] Donald Beaver. Efficient multiparty protocols using circuit randomization. In *Annual International Cryptology Conference*, pages 420–432. Springer, 1991.

[10] Elie Bursztein et al. Rethinking the detection of child sexual abuse imagery on the internet. In *The World Wide Web Conference*, 2019.

[11] Jon Callas. Thoughts on mitigating abuse in an end-to-end. Technical report, Stanford University, 2020.

[12] Konstantinos Chatzikokolakis, Giovanni Cherubin, Catuscia Palamidessi, and Carmela Troncoso. The bayes security measure, 2020.

[13] Hao Chen, Ilaria Chillotti, Yihe Dong, Oxana Poburinnaya, Ilya Razenshteyn, and M Sadegh Riazi. {SANNS}: Scaling up secure approximate k-nearest neighbors search. In *29th USENIX Security Symposium (USENIX Security 20)*, 2020.

[14] Benny Chor, Oded Goldreich, Eyal Kushilevitz, and Madhu Sudan. Private information retrieval. In *Proceedings of IEEE 36th Annual Foundations of Computer Science*, pages 41–50. IEEE, 1995.

[15] Ondrej Chum, James Philbin, Andrew Zisserman, et al. Near duplicate image detection: min-hash and tf-idf weighting. In *Proceedings of the British Machine Conference, pages*, volume 810, pages 812–815, 2008.

[16] Harris Cohen. Bringing fact check information to google images. Technical report, Google, 2020.

[17] Corinna Cortes and Mehryar Mohri. Auc optimization vs. error rate minimization. In *Advances in Neural Information Processing Systems*, pages 313–320, 2004.

[18] Andrew Crocker and Gennie Gebhart. Don't let encrypted messaging become a hollow promise. *Electronic Frontier Foundation*, 2020.

[19] Jesse Davis and Mark Goadrich. The relationship between precision-recall and roc curves. In *Proceedings of the 23rd International Conference on Machine Learning*, pages 233–240, 2006.

[20] Yevgeniy Dodis, Leonid Reyzin, and Adam Smith. Fuzzy extractors: How to generate strong keys from biometrics and other noisy data. In *International Conference on the Theory and Applications of Cryptographic Techniques*, pages 523–540. Springer, 2004.

[21] Maeve Duggan. *Online harassment*. Pew Research Center, 2017.

[22] Cynthia Dwork. Differential privacy: A survey of results. In *International conference on theory and applications of models of computation*, pages 1–19. Springer, 2008.

[23] Encryption working group. Moving the encryption policy conversation forward. *Carnegie Endowment for International Peace*, 2019.

[24] Zekeriya Erkin, Martin Franz, Jorge Guajardo, Stefan Katzenbeisser, Inald Lagendijk, and Tomas Toft. Privacy-preserving face recognition. In *International Symposium on Privacy Enhancing Technologies Symposium*, pages 235–253. Springer, 2009.

[25] David Evans, Yan Huang, Jonathan Katz, and Lior Malka. Efficient privacy-preserving biometric identification. In *Proceedings of the 17th conference Network and Distributed System Security Symposium, NDSS*, volume 68, 2011.

[26] Facebook. Applying to ThreatExchange. https://developers.facebook.com/programs/threatexchange/, 2019. Accessed Jun 2020.

[27] Armando Faz-Hernández and Kris Kwiatkowski. *Introducing CIRCL: An Advanced Cryptographic Library*. Cloudflare, June 2019. Available at https://github.com/cloudflare/circl. Accessed Feb 2021.

[28] Vijaya Gadde and Yoel Roth. Enabling further research of information operations on twitter. https://blog.twitter.com/en_us/topics/company/2018/enabling-further-research-of-information-operations-on-twitter.html. Accessed April 2021.

[29] Aristides Gionis, Piotr Indyk, Rajeev Motwani, et al. Similarity search in high dimensions via hashing. In *Proceedings of 25th International Conference on Very Large Data Bases*, volume 99, pages 518–529, 1999.

[30] Shafi Goldwasser and Silvio Micali. Probabilistic encryption. *Journal of Computer and System Sciences*, 28(2):270–299, 1984.

[31] Matthew Green and Alex Stamos. Apple wants to protect children. but it's creating serious privacy risks. *New York Times*, 2021.

[32] Jacob Gursky and Samuel Woolley. Countering disinformation and protecting democratic communication on encrypted messaging applications. 2021.

[33] Matthew Hindman. *Disinformation, Fake News and Influence Campaigns on Twitter*. John S. and James L. Knight Foundation, 2018.

[34] Yiqing Hua, Mor Naaman, and Thomas Ristenpart. Characterizing twitter users who engage in adversarial interactions against political candidates. In *Proceedings of the 2020 CHI Conference on Human Factors in Computing Systems*, pages 1–13, 2020.

[35] Yiqing Hua, Armin Namavari, Kaishuo Cheng, Mor Naaman, and Thomas Ristenpart. Increasing adversarial uncertainty to scale private similarity testing. *arXiv preprint arXiv:2109.01727*, 2021.

[36] Yiqing Hua, Thomas Ristenpart, and Mor Naaman. Towards measuring adversarial twitter interactions against candidates in the us midterm elections. In *Proceedings of the International AAAI Conference on Web and Social Media*, volume 14, pages 272–282, 2020.

[37] Ayman Jarrous and Benny Pinkas. Secure computation of functionalities based on hamming distance and its application to computing document similarity. *International Journal of Applied Cryptography*, 2013.

[38] Ari Juels and Martin Wattenberg. A fuzzy commitment scheme. In *Proceedings of the 6th ACM Conference on Computer and Communications Security*, 1999.

[39] Ben Kaiser, Jerry Wei, Elena Lucherini, Kevin Lee, J Nathan Matias, and Jonathan Mayer. Adapting security warnings to counter online disinformation. In *30th USENIX Security Symposium (USENIX Security 21)*, 2021.

[40] Mallory Knodel. New technical report brings together experts to tackle encryption myths. *Center for Democracy & Technology*, 2020.

[41] B. Knott, S. Venkataraman, A.Y. Hannun, S. Sengupta, M. Ibrahim, and L.J.P. van der Maaten. Crypten: Secure multi-party computation meets machine learning. In *Proceedings of the NeurIPS Workshop on Privacy-Preserving Machine Learning*, 2020.

[42] Anunay Kulshrestha and Jonathan Mayer. Identifying harmful media in end-to-end encrypted communication: Efficient private membership computation. In *30th USENIX Security Symposium (USENIX Security 21)*, 2021.

[43] Lucy Li, Bijeeta Pal, Junade Ali, Nick Sullivan, Rahul Chatterjee, and Thomas Ristenpart. Protocols for checking compromised credentials. In *Proceedings of the 2019 ACM SIGSAC Conference on Computer and Communications Security*, pages 1387–1403, 2019.

[44] Wen Li, Limin Wang, Wei Li, Eirikur Agustsson, and Luc Van Gool. Webvision database: Visual learning and understanding from web data. *arXiv preprint arXiv:1708.02862*, 2017.

[45] Tsung-Yi Lin, Michael Maire, Serge Belongie, James Hays, Pietro Perona, Deva Ramanan, Piotr Dollár, and C Lawrence Zitnick. Microsoft coco: Common objects in context. In *European Conference on Computer Vision*, pages 740–755. Springer, 2014.

[46] Wenjun Lu, Ashwin Swaminathan, Avinash L Varna, and Min Wu. Enabling search over encrypted multimedia databases. In *Media Forensics and Security*, volume 7254, page 725418. International Society for Optics and Photonics, 2009.

[47] Christopher Manning and Hinrich Schutze. *Foundations of statistical natural language processing*. MIT press, 1999.

[48] J Matias, Amy Johnson, Whitney Erin Boesel, Brian Keegan, Jaclyn Friedman, and Charlie DeTar. Reporting, reviewing, and responding to harassment on twitter. *Available at SSRN 2602018*, 2015.

[49] Jonathan Mayer. Content moderation for end-to-end encrypted messaging. *Princeton University*, 2019.

[50] India Mckinney and Erica Potnoy. Apple's plan to "think different" about encryption opens a backdoor to your private life. *The Electronic Frontier Foundation*, 2021.

[51] Microsoft. PhotoDNA. https://www.microsoft.com/en-us/photodna, 2020. Accessed July 2020.

[52] Alec Muffet. What do we mean by a "backdoor" in end-to-end encrypted messengers or secure messengers? #endtoendencryption #e2ee. https://alecmuffett.com/article/14275, 2021. Accessed May 2021.

[53] Mohammad Norouzi, Ali Punjani, and David J Fleet. Fast search in hamming space with multi-index hashing. In *2012 IEEE conference on computer vision and pattern recognition*, pages 3108–3115. IEEE, 2012.

[54] Aude Oliva and Antonio Torralba. Modeling the shape of the scene: A holistic representation of the spatial envelope. *International Journal of Computer Vision*, 42(3):145–175, 2001.

[55] Simon Oya, Carmela Troncoso, and Fernando Pérez-González. Is geo-indistinguishability what you are looking for? WPES '17, page 137–140, New York, NY, USA, 2017. Association for Computing Machinery.

[56] Pascal Paillier. Public-key cryptosystems based on composite degree residuosity classes. In *International conference on the theory and applications of cryptographic techniques*, pages 223–238. Springer, 1999.

[57] Erica Potnoy. Why adding client-side scanning breaks end-to-end encryption. *The Electronic Frontier Foundation*, 2019.

[58] Vijay Raghavan, Peter Bollmann, and Gwang S Jung. A critical investigation of recall and precision as measures of retrieval system performance. *ACM Transactions on Information Systems (TOIS)*, 7(3):205–229, 1989.

[59] Gustavo Resende et al. (mis) information dissemination in whatsapp: Gathering, analyzing and countermeasures. In *The World Wide Web Conference*, 2019.

[60] M Sadegh Riazi, Beidi Chen, Anshumali Shrivastava, Dan Wallach, and Farinaz Koushanfar. Sub-linear privacy-preserving near-neighbor search. *arXiv preprint arXiv:1612.01835*, 2016.

[61] Rasmus Rothe, Radu Timofte, and Luc Van Gool. Dex: Deep expectation of apparent age from a single image. In *IEEE International Conference on Computer Vision Workshops (ICCVW)*, December 2015.

[62] Rasmus Rothe, Radu Timofte, and Luc Van Gool. Deep expectation of real and apparent age from a single image without facial landmarks. *International Journal of Computer Vision*, 126(2-4):144–157, 2018.

[63] Z. Alan Rozenshtein. Child exploitation and the future of encryption. *LAWFARE Blog*, 2019.

[64] Ahmad-Reza Sadeghi, Thomas Schneider, and Immo Wehrenberg. Efficient privacy-preserving face recognition. In *International Conference on Information Security and Cryptology*, pages 229–244. Springer, 2009.

[65] Takaya Saito and Marc Rehmsmeier. The precision-recall plot is more informative than the roc plot when evaluating binary classifiers on imbalanced datasets. *PLoS ONE*, 10(3):e0118432, 2015.

[66] Jagarlamudi Shashank, Palivela Kowshik, Kannan Srinathan, and CV Jawahar. Private content based image

retrieval. In *2008 IEEE Conference on Computer Vision and Pattern Recognition*, pages 1–8. IEEE, 2008.

[67] Reza Shokri, George Theodorakopoulos, Jean-Yves Le Boudec, and Jean-Pierre Hubaux. Quantifying location privacy. In *2011 IEEE Symposium on Security and Privacy*, pages 247–262, 2011.

[68] Reza Shokri, George Theodorakopoulos, Carmela Troncoso, Jean-Pierre Hubaux, and Jean-Yves Le Boudec. Protecting location privacy: Optimal strategy against localization attacks. In *Proceedings of the 2012 ACM Conference on Computer and Communications Security*, CCS '12, page 617–627, New York, NY, USA, 2012. Association for Computing Machinery.

[69] Catherine Shu and Jonathan Shieber. Facebook, reddit, google, linkedin, microsoft, twitter and youtube issue joint statement on misinformation. *Tech Crunch*, 2020.

[70] Kurt Thomas et al. Protecting accounts from credential stuffing with password breach alerting. In *28th USENIX Security Symposium (USENIX Security 19)*, pages 1556–1571, 2019.

[71] Lucia Vadicamo et al. Cross-media learning for image sentiment analysis in the wild. In *2017 IEEE International Conference on Computer Vision Workshops (ICCVW)*, pages 308–317, Oct 2017.

[72] Xiao Wang, Alex J. Malozemoff, and Jonathan Katz. EMP-toolkit: Efficient MultiParty computation toolkit. https://github.com/emp-toolkit, 2016.

[73] Caitlin Webb and Sally Weale. More than 500 child victims of 'revenge porn' in england and wales last year. *The Guardian*, 2020.

[74] WhatsApp. Stopping abuse: How whatsapp fights bulk messaging and automated behavior. Technical report, 2018.

[75] Zhihua Xia, Xinhui Wang, Liangao Zhang, Zhan Qin, Xingming Sun, and Kui Ren. A privacy-preserving and copy-deterrence content-based image retrieval scheme in cloud computing. *IEEE Transactions on Information Forensics and Security*, 11(11):2594–2608, 2016.

[76] Qixue Xiao, Yufei Chen, Chao Shen, Yu Chen, and Kang Li. Seeing is not believing: Camouflage attacks on image scaling algorithms. In *28th USENIX Security Symposium (USENIX Security 19)*, 2019.

[77] Andrew Chi-Chih Yao. How to generate and exchange secrets. In *27th Annual Symposium on Foundations of Computer Science*, pages 162–167. IEEE, 1986.

[78] Christoph Zauner. Implementation and benchmarking of perceptual image hash functions. 2010.